31st Congress of the International Council of the Aeronautical Sciences

Belo Horizonte, Brazil; September 09-14, 2018

EULERIAN OPTIMAL CONTROL FORMULATION FOR DYNAMIC MORPHING OF AIRSPACE SECTORS

Yixiang Lim*, Niveditha Premlal*, Alessandro Gardi* and Roberto Sabatini*
***RMIT University – School of Engineering, Bundoora, VIC 3083, Australia**

Keywords: Dynamic airspace, air traffic flow management, trajectory-based operations

Abstract

The steadily increasing air traffic demand has highlighted a need to evolve existing Air Traffic Flow Management (ATFM) methodologies by increasing automation support in airborne and ground-based systems and more flexible modulation of air traffic controller workload. Dynamic Airspace Management (DAM) aims at optimising the demand-capacity balance in all airspace regions at all times with a particular focus on capacity modulation measures. In this paper, we propose a novel DAM approach supporting the dynamic morphing of airspace sector boundaries based on an optimal-control formulation. The Eulerian continuity principle is used to model the air traffic flow at a macroscopic scale and workload-based capacity constraints are considered to determine the optimal variations in sector volumes. The demand levels are determined and the traffic flow theory based on the principle of continuity is used to propagate the demand across airspace sectors, approximated as 2D polygons. The newly developed sector morphing framework will be integrated into next-generation ATFM decision support systems to drive adaptive human-machine interfaces and interactions supporting more efficient exploitation of airspace resources.

1 Introduction

In parallel with the increasing adoption of automated airborne and ground-based systems for planning, exchange, negotiation and validation of 4-Dimensional Trajectory (4DT) intents to resolve traffic conflicts and avoid hazardous areas and weather cells, the avionics and Air Traffic Management (ATM) research community has identified an important need to concurrently evolve the Air Traffic Flow Management (ATFM) and Airspace Management (ASM) methodologies and technologies. Both ATFM and ASM fundamentally aim at optimising the Demand-Capacity Balance (DCB) at all times and in all airspace regions, but traditional ATFM strategies focus on modulating the demand, whereas Dynamic Airspace Management (DAM) was specially shortlisted as a promising ASM evolution pathway due to its focus on capacity modulation measures [1, 2]. DAM concepts can be classified based on the kind of modulation, which can address time-only, space-only (2D/3D) or space-time (4D). While discrete-time strategic and tactical modulation measures are already being implemented in ATFM/ASM and also captured as part of the so-called Flexible Use of Airspace (FUA) [3], tactical space and space-time modulations for DAM are subjects of currently active research [4-10]. Space and space-time modulations are particularly expected to realise the morphing concept as conceptually depicted in Fig. 1.

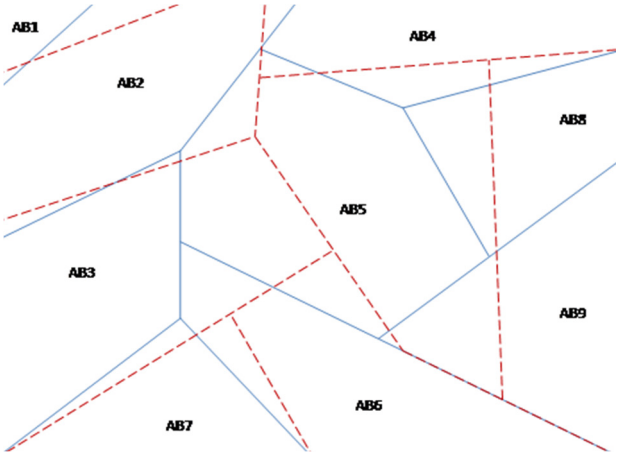

Fig. 1. DAM space adaptation principle [2].

However, previous DAM research has given limited consideration to the dynamical factors driving this modulation, which shall be unsteady and non-isotropic in nature to be able to drive an effective space-time adaptation [2, 11, 12]. Considering its significant implications, DAM has the potential to be paradigm shift in aviation, capable of both accommodating the traffic demand trends of the future and to synergistically mitigate the effects that unforeseen perturbations have on the nominal capacities, which can easily lead to greater disruptions on wider regions of airspace.

Additionally, in order to support unrestricted access of Unmanned Aircraft Systems (UAS) to all classes of airspace, it will be essential to transition to a dynamic management of airspace resources, capturing the sometimes competing demands of manned civil and military aircraft as well as unmanned aircraft.

The research presented in this paper aims at establishing a powerful analytical framework combining 4D trajectory management models for ATM/ATFM to drive dynamic (4D) airspace adaptation towards an optimal DCB in all classes of airspace and in all possible airspace configurations.

2 Mathematical Models

The Lighthill-Witham-Richards (LWR) model has been extensively employed in road traffic dynamics studies. This Eulerian approach efficiently models the traffic flow as a continuum, which is an accurate approximation at the macroscopic scale. The continuity equation at the core of these methods is a linear partial differential equation that can be applied in discretised form to various airway segments.

This approach was successfully demonstrated by Work and Bayen [13], which used an Eulerian model for flow prediction and to determine speed control measures.

Generalised Continuity Equation

The generalised continuity equation is applied to model the flow of air traffic within a given airspace, assumed to be a finite control volume which is fixed in space. The flow is assumed to be inviscid, incompressible and irrotational, yielding a very simple yet accurate approximation, as demonstrated in various road studies [14]. The flux of aircraft into and out of the control volume is given as a function of time, with inflows considered to be negative and outflows considered to be positive. The generalized continuity equation can be expressed in differential form as:

$$\frac{\partial \rho}{\partial t} + \nabla \cdot (\rho \boldsymbol{v}) = 0 \qquad (1)$$

where ρ is the air traffic density (aircraft count per NM^3), $\boldsymbol{v}$ is mean air traffic flow velocity (kts) such that $\rho\boldsymbol{v}$ is the flux (aircraft count per NM^2 hour). Assuming incompressibility ($\nabla \cdot \boldsymbol{v} = 0$), and defining a flow potential φ such that $\boldsymbol{v} = \nabla\varphi$, Eq (1) can re-written as:

$$\frac{\partial \rho}{\partial t} + \nabla\varphi \cdot \nabla\rho = 0 \qquad (2)$$

Additionally, for an arbitrary element i within the control volume, the rate of change of the element's aircraft count is given according to the following equation:

$$\begin{aligned} \frac{\partial n_i}{\partial t} &= \frac{\partial (\rho_i V_i)}{\partial t} \\ &= V_i \frac{\partial \rho_i}{\partial t} + \rho_i \frac{\partial V_i}{\partial t} \end{aligned} \qquad (3)$$

where n_i is the aircraft count, and ρ_i and V_i are respectively the air traffic density and volume (NM^3) of element i. Rearranging Eq (3) and substituting into Eq (2), one obtains the continuity equation as applied to element i:

$$\frac{1}{V_i}\left(\frac{\partial n_i}{\partial t} - \rho_i \frac{\partial V_i}{\partial t}\right) + \nabla\varphi_i \cdot \nabla\rho_i = 0 \qquad (4)$$

where the subscript i is used to denote properties belonging to element i. Finally, multiplying throughout by the element volume, one obtains:

$$\frac{\partial n_i}{\partial t} - \rho_i \frac{\partial V_i}{\partial t} + V_i(\nabla\varphi_i \cdot \nabla\rho_i) = 0 \qquad (5)$$

Optimal Control Formulation

Eq (5) can be formulated as an optimal control problem by considering a control volume with 4-D fields $\rho(x, y, z, t)$ and $\varphi(x, y, z, t)$ and containing I sectors. The system dynamics are given by:

$$\boldsymbol{x} \triangleq \begin{cases} x_i = n_i, & i \in [1, \dots, I] \\ x_j = V_i, & j \in [I+1, \dots, 2I] \end{cases} \qquad (6)$$

$$\boldsymbol{u} \triangleq \{\dot{V}_i\}, \qquad i \in [1, \dots, I] \tag{7}$$

$$\dot{\boldsymbol{x}} \triangleq \begin{cases} \dot{x}_i = \rho_i u_i - x_j(\nabla\varphi_i \cdot \rho_i), \\ \dot{x}_j = u_i \end{cases} \tag{8}$$

Minimising the cost function:

$$J = \sum_{i=1}^{I} (18 - \bar{n}_i)^2 \tag{9}$$

where $\bar{n}_i$ is the time-averaged aircraft count in element i, and subject to the constraints

$$9 \le x_i \le 18, \qquad \forall\, i \in [1, \dots, I] \tag{10}$$

$$x_j \ge 4630\ NM^3, \quad \forall\, j \in [I+1, \dots, 2I] \tag{11}$$

$$-926\ NM^3 h^{-1} \le u_i \le 926\ NM^3 h^{-1} \quad \forall\, i \in [1, \dots, I] \tag{12}$$

Eq (10) is specified to ensure that the traffic load for each sector remains between 50% and 100%. Eq (11) is calculated as the square of the minimum sector characteristic dimension multiplied by an altitude of 5000 ft. The minimum characteristic dimension is the one corresponding to a transit time of approximately 11 minutes, which marks the transition from the maximum number of aircraft constraint to the maximum throughput constraint in the Federal Aviation Administration (FAA) Monitor Alert Parameter (MAP) model [11]. Eq. (12) is a heuristic constraint introduced to prevent excessively abrupt changes in the sector volume and is set to ±20% of the minimum volume per hour.

3 Airspace Pre-Partitioning

The formulation presented in the previous section is not designed for a complete partitioning of the initial control volume. As such, the first step towards a practical implementation of the theory presented in the previous section lies in an efficient clustering of initial sectors. A heuristic approach is presented which determines the initial number of sectors and their respective locations. The algorithm is presented in Fig. 2.

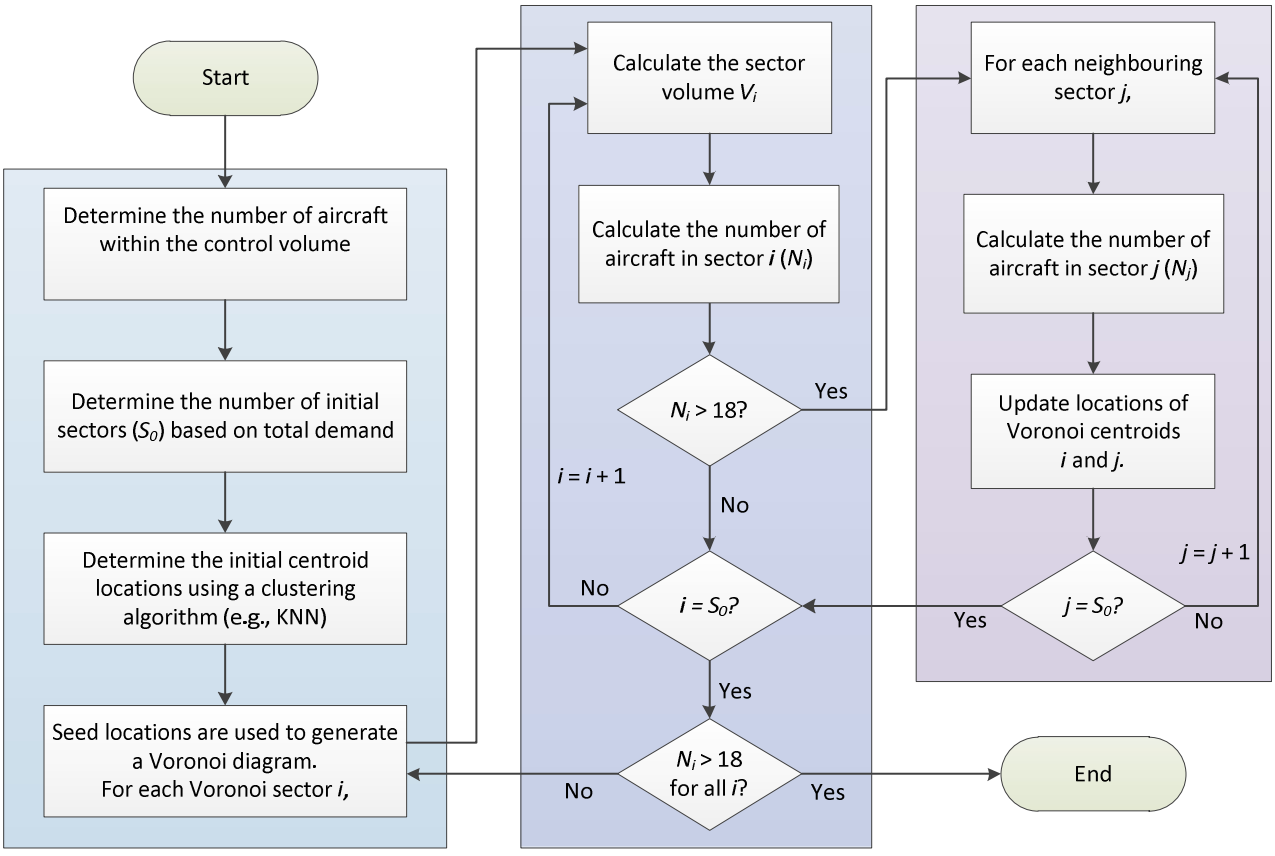

Fig. 2. Pre-partitioning algorithm process.

The aircraft count over the entire control volume is first computed from the air traffic density. As the number of aircraft in the control volume changes over time as a function of the air traffic density, the peak count occurring at time t_k is used to determine the maximum number of sectors required. A clustering algorithm such as the k-nearest neighbours (KNN) can then be used to determine the seed location of the initial sectors, which are used to partition the control volume into Voronoi diagrams. Each Voronoi diagram constitutes a sector of airspace. A check is then conducted on all sectors to ensure that the aircraft count does not exceed the maximum limit of 18. For sectors exceeding this limit, the seed locations are moved in the direction of decreasing density. The translation is determined by comparing the aircraft count in neighbouring sectors; a sector with a lower aircraft count will expand towards one with a higher aircraft count, causing the latter to shrink.

The result of the pre-partioning algorithm is illustrated in Fig. 3, with over- or under-loaded sectors color-coded with higher opacity. The initial partitioning performs reasonably well for a wide range of different control volumes while producing convex sector shapes and, when no initial sector configuration is specified, it can be used to generate an initial sector configuration as input for the sector morphing algorithm described in Section 2. The morphing algorithm then propagates the morphing of the initial sector configuration forwards and backwards in time for the desired time-frame.

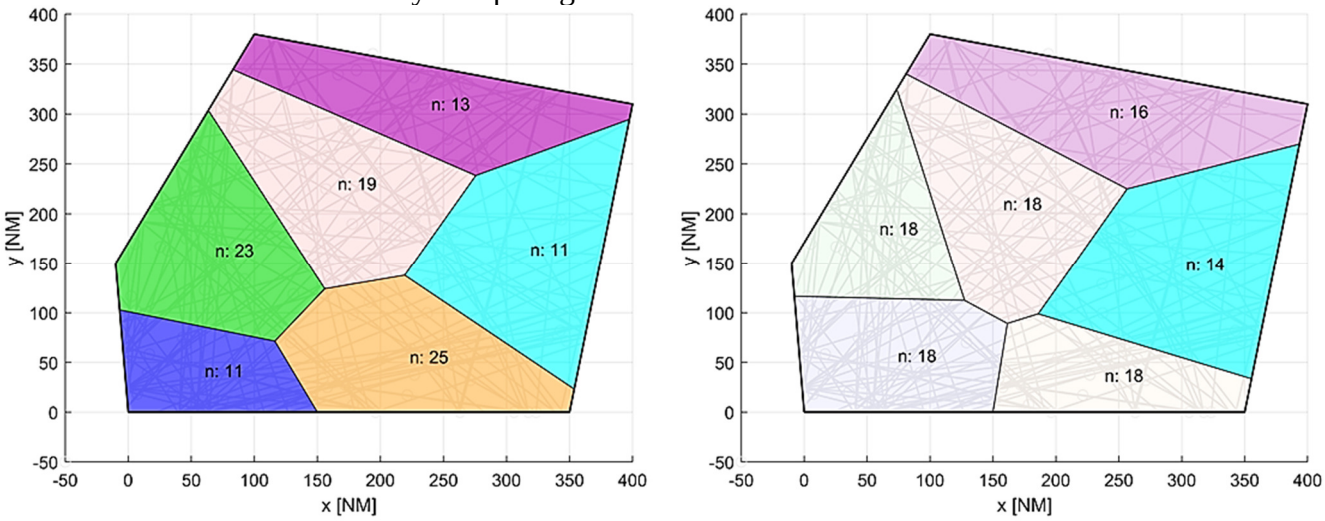

Fig. 3. Results of pre-partitioning algorithm. The figure on the left shows the sectors generated by initial clustering and the figure on the right shows the sectors generated by iterative movement of the Voronoi centroids

4 Morphing Algorithm

The control parameter $\dot{\boldsymbol{V}} = [\dot{V}_1, \dots, \dot{V}_I]^T$ is used to control the sector morphing by updating the position of airspace nodes, which are the intersections between different sector edges as well as the airspace boundary. Given an airspace configuration containing I sectors and J nodes, a system of equations can be established as:

$$\boldsymbol{A} \cdot \boldsymbol{x} = \boldsymbol{b} \tag{13}$$

where $\boldsymbol{x}_{2J\times 1} = [x_1, y_1, x_2, y_2, \dots, x_J, y_J]^T$ is the node translation matrix containing the x and y coordinates describing the translation of all nodes; $\boldsymbol{A} = \begin{bmatrix} \boldsymbol{A1} \\ \boldsymbol{A2} \end{bmatrix}$ contains the inflation matrix $\boldsymbol{A1}_{I\times 2J}$ which describes the change in volume of sector i when node j is perturbed by a unit vector in the x- and y-directions, and the boundary constraint matrix $\boldsymbol{A2}_{J_b\times 2J}$ which contains constraints on the movement of boundary nodes. Fig. 4 illustrates the method used to determine the coefficients of $\boldsymbol{A1}$.

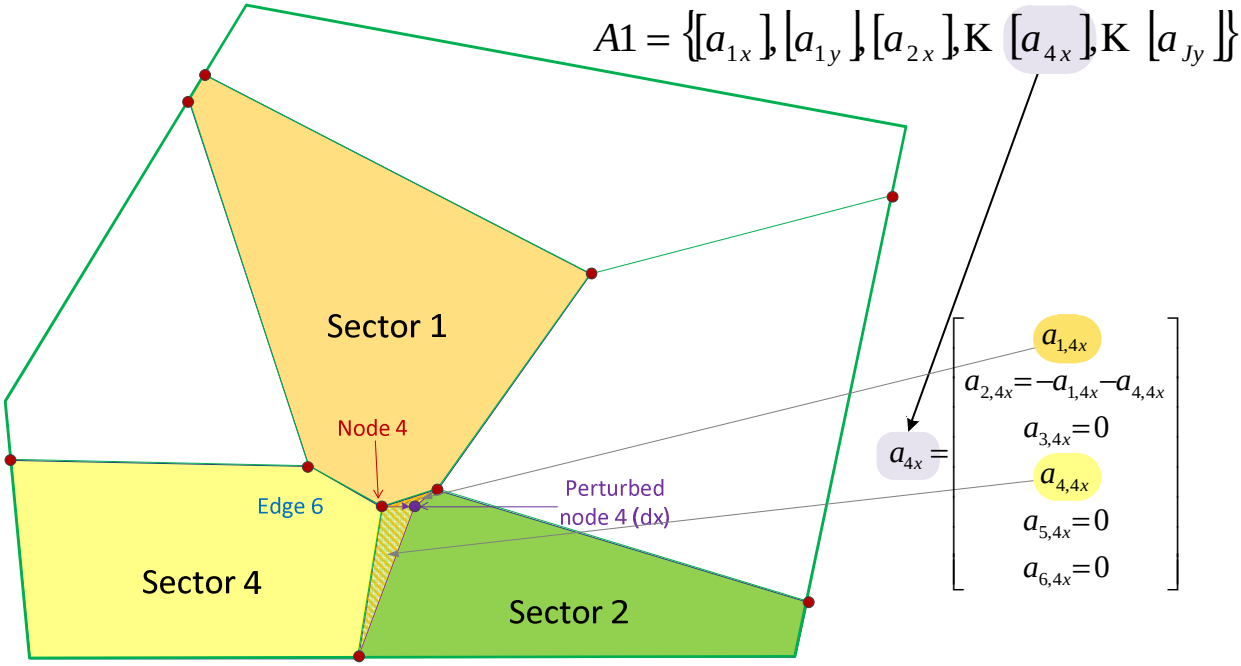

Fig. 4. Method for determining the coefficients of inflation matrix ***A1***.

Node j is perturbed by unit vectors in the x and y directions to obtain a vector containing the volume changes of each sector due to this perturbation. This process is iterated through all nodes. The vector $\boldsymbol{b} = \begin{bmatrix} \boldsymbol{b1} \\ \boldsymbol{b2} \end{bmatrix}$ contains $\boldsymbol{b1}_{I\times 1} = [\Delta\tilde{V}_1, \Delta\tilde{V}_2, \dots, \Delta\tilde{V}_I]^T$, the vector of normalised inflation in each sector and $\boldsymbol{b2}_{J_b\times 1} = [\emptyset]$, the boundary constraint vector. $\boldsymbol{b1}$ is obtained by integrating the normalised control parameter $\dot{\tilde{\boldsymbol{V}}}$ over time – $\dot{\tilde{\boldsymbol{V}}}_{\boldsymbol{i}}$, in turn, can obtained from normalising $\dot{\boldsymbol{V}}$ with respect to each sector's relative volume such that the inflation in all sectors is equal to zero:

$$\sum_I \dot{\tilde{V}}_i = \sum_I \left(\dot{V}_i - \Lambda_i\right) = 0 \qquad (14)$$

$$where\ \Lambda_i = \frac{V_i \cdot \sum_I \dot{V}_i}{\sum_I V}$$

The morphing algorithm is illustrated in Fig. 5. At a specified time epoch, the control parameter $\dot{\boldsymbol{V}}$ is given by the solution the optimal control problem and is normalised and integrated to obtain $\boldsymbol{b}$. At the same time, the sector and node parameters are extracted from the existing sector configuration and used in generating the $\boldsymbol{A}$ matrix. As the actual inflation of the sectors do not scale linearly with translations in x and y, (i.e., $\boldsymbol{A1}$ is an approximation of the actual inflation and is accurate only for small perturbations about the nodes), the actual node translations are computed in a stepwise iterative manner. This is achieved by subdividing $\boldsymbol{b1}$ into intervals such that the sector inflation at each interval does not exceed a given threshold. The solution of $\boldsymbol{x}$ obtained at each interval is used to update the sector configuration and regenerate $\boldsymbol{A1}$ and $\boldsymbol{b1}$ for the subsequent iteration. The morphing results are shown in Fig. 6.

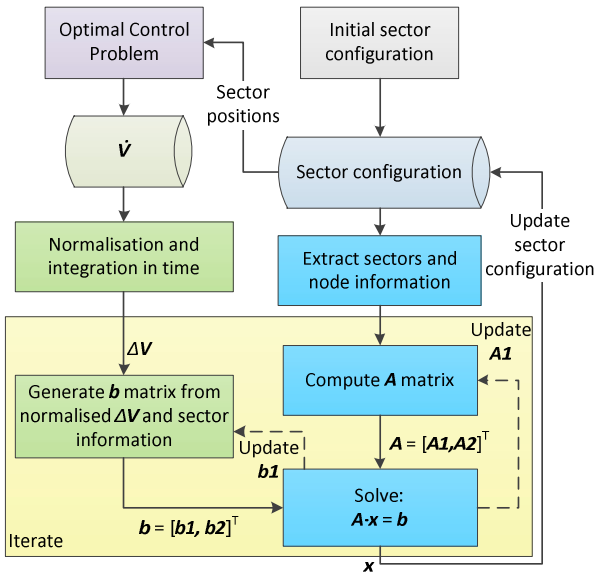

Fig. 5. Sector morphing algorithm.

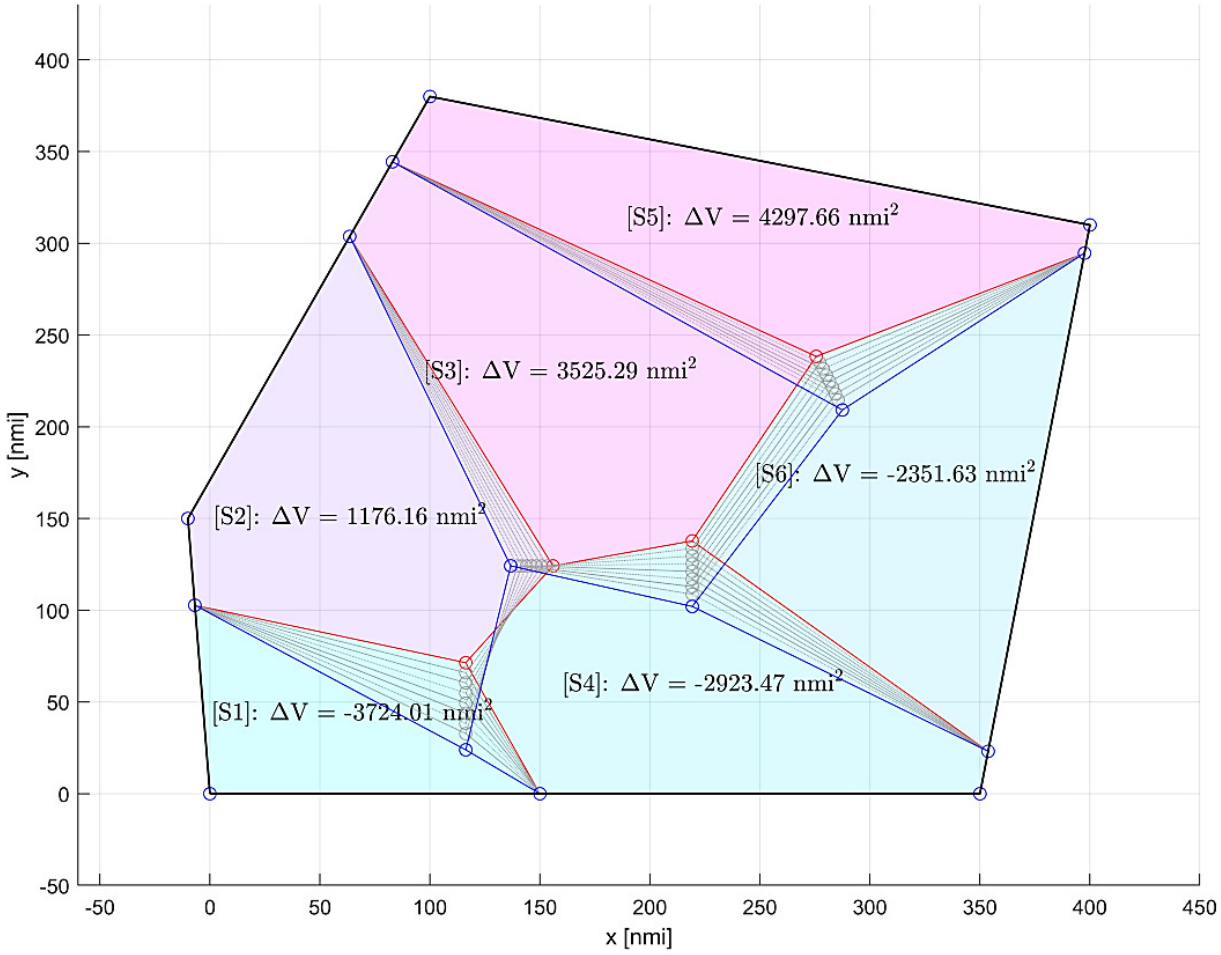

Fig. 6. Results of morphing algorithm. Sectors are colour-coded according to the determined volume variations, with negative being blue.

Fairly large values of $\dot{\boldsymbol{V}}$ were generated to exaggerate the change in sector sizes. As shown in the figure, the algorithm successfully computes the required node translation to achieve the specified normalised volume changes. Although the boundary nodes were constrained by ***A2*** and ***b2*** such that they could move, but only along the boundary of the airspace (effectively preserving the shape and size of the airspace), the algorithm prefers to move the interior nodes to achieve the required volume changes. The relative error of the morphing process, defined as the relative difference between the expected inflation and inflation achieved through morphing (i.e., $\varepsilon_i = \frac{|\Delta\tilde{V}_i - \Delta V_i|}{\Delta\tilde{V}_i}$), was very small, with the maximum error $\varepsilon_{max} = \max_{i=1\ldots I} \varepsilon_i$ being in the order of 10^{-6}.

4 Conclusion

This paper addressed the important problem of morphing sector boundaries to support dynamic modulation of airspace capacity. Similarly to road traffic flow dynamics studies, a fully dynamic problem was posed by assuming macroscopic continuity of air traffic across large airspace regions. This allowed for a suitably-derived Eulerian flow theory to be exploited to model individual sector densities over time. The obtained set of differential equations was subsequently used to formulate the sector morphing as an optimal control problem, with the number of aircraft in each sector and their volumes as the state variables and the volume variation in each sector as control variables. To translate these volume variations into the morphing of sector boundaries, a system of linear equations was derived based on geometric

considerations. Suitable constraints on vertex movements were introduced to reduce the solution space. The exact solution (in terms of vertex movements to satisfy the desired sector volume variations) is computed iteratively, yielding a convergence with very low relative error (in the order of 10^{-6}) as demonstrated through an initial case study in representative conditions.

References

[1] R. Sabatini, A. Gardi, S. Ramasamy, T. Kistan, and M. Marino, "Modern Avionics and ATM Systems for Green Operations," in *Encyclopedia of Aerospace Engineering*, R. Blockley and W. Shyy, Eds., ed: John Wiley & Sons, 2015.

[2] T. Kistan, A. Gardi, R. Sabatini, S. Ramasamy, and E. Batuwangala, "An evolutionary outlook of air traffic flow management techniques," *Progress in Aerospace Sciences*, vol. 88, pp. 15-42, 2017.

[3] EUROCONTROL, "European Route Network Improvement Plan - Part 3: Airspace Management Handbook - Guidelines for Airspace Management", EUROCONTROL,, Brussels, Belgium, November, 2017.

[4] S. A. Martinez, G. B. Chatterji, D. Sun, and A. M. Bayen, "A weighted-graph approach for dynamic airspace configuration," *AIAA Guidance, Navigation, and Control Conference 2007*, Hilton Head, SC, 2007, pp. 1476-1491.

[5] P. Cheng and R. Geng, "Dynamic Airspace Management - Models and Algorithms," in *Air Traffic Control*, M. Mulder, Ed., ed: InTech, 2010.

[6] H. D. Sherali and J. M. Hill, "Configuration of airspace sectors for balancing air traffic controller workload," *Annals of Operations Research*, vol. 203, pp. 3-31, 2011.

[7] J. Tang, S. Alam, C. Lokan, and H. A. Abbass, "A multi-objective approach for Dynamic Airspace Sectorization using agent based and geometric models," *Transportation Research Part C: Emerging Technologies*, vol. 21, pp. 89-121, 2012.

[8] Y. Chen, H. Bi, D. Zhang, and Z. Song, "Dynamic airspace sectorization via improved genetic algorithm," *Journal of Modern Transportation*, vol. 21, pp. 117-124, 2013.

[9] M. Bloem, M. Drew, C. F. Lai, and K. D. Bilimoria, "Advisory algorithm for scheduling open sectors, operating positions, and workstations," *Journal of Guidance, Control, and Dynamics*, vol. 37, pp. 1158-1169, 2014.

[10] Y. Chen and D. Zhang, "Dynamic airspace configuration method based on a weighted graph model," *Chinese Journal of Aeronautics*, vol. 27, pp. 903-912, 2014.

[11] J. D. Welch, J. Y. N. Cho, N. K. Underhill, and R. A. DeLaura, "Sector workload model for benefits analysis and convective weather capacity prediction," *10th USA/Europe ATM R&D Seminar, ATM 2013*, 2013.

[12] J. D. Welch, J. W. Andrews, B. D. Martin, and B. Sridhar, "Macroscopic workload model for estimating en route sector capacity," *7th USA/Europe ATM Research and Development Seminar, ATM2007*, Barcelona, Spain, 2007.

[13] D. B. Work and A. M. Bayen, "Convex Formulations of Air Traffic Flow Optimization Problems," *Proceedings of the IEEE*, vol. 96, pp. 2096-2112, 2008.

[14] M. Treiber and A. Kesting Eds., *Traffic Flow Dynamics*, Springer-Verlag, Berlin, Germany, 2013.

Copyright Statement